



Sulfur Deficiency-Induced Glucosinolate Catabolism Attributed to Two β -Glucosidases, BGLU28 and BGLU30, is Required for Plant Growth Maintenance under Sulfur Deficiency

Liu Zhang¹, Ryota Kawaguchi¹, Tomomi Morikawa-Ichinose¹, Alaa Allaham ¹, Sun-Ju Kim² and Akiko Maruyama-Nakashita ^{1,*}

¹Department of Bioscience and Biotechnology, Faculty of Agriculture, Kyushu University, 744 Motooka, Nishi-ku, Fukuoka, 819-0395 Japan

²Department of Bio-Environmental Chemistry, College of Agriculture and Life Sciences, Chungnam National University, Daejeon 34134, South Korea

*Corresponding author: E-mail, amaru@agr.kyushu-u.ac.jp; Fax, +81-92-802-4712.

(Received October 27, 2019; Accepted January 21, 2020)

Sulfur (S) is an essential element for plants, and S deficiency causes severe growth retardation. Although the catabolic process of glucosinolates (GSLs), the major S-containing metabolites specific to *Brassicales* including *Arabidopsis*, has been recognized as one of the S deficiency (–S) responses in plants, the physiological function of this metabolic process is not clear. Two β -glucosidases (BGLUs), BGLU28 and BGLU30, are assumed to be responsible for this catabolic process as their transcript levels were highly upregulated by –S. To clarify the physiological function of BGLU28 and BGLU30 and their roles in GSL catabolism, we analyzed the accumulation of GSLs and other S-containing compounds in the single and double mutant lines of BGLU28 and BGLU30 and in wild-type plants under different S conditions. GSL levels were highly increased, while the levels of sulfate, cysteine, glutathione and protein were decreased in the double mutant line of BGLU28 and BGLU30 (*bglu28/30*) under –S. Furthermore, transcript level of *Sulfate Transporter1;2*, the main contributor of sulfate uptake from the environment, was increased in *bglu28/30* mutants under –S. With these metabolic and transcriptional changes, *bglu28/30* mutants displayed obvious growth retardation under –S. Overall, our results indicate that BGLU28 and BGLU30 are required for –S-induced GSL catabolism and contribute to sustained plant growth under –S by recycling sulfate to primary S metabolism.

Keywords: *Arabidopsis thaliana* • β -Glucosidases • Glucosinolates • Glucosinolate catabolism • Plant growth • Sulfur deficiency.

Introduction

Sulfur (S) is an essential macronutrient for plant growth and development. The main source of S in the environment is inorganic sulfate. Sulfate can be absorbed by plants through the function of sulfate transporters and further assimilated into

organic S compounds in plants (Takahashi et al. 2011, Long et al. 2015). Cysteine is the first compound containing reduced S in the S assimilation pathway and serves as a precursor for other organic S compounds, such as methionine and glutathione (GSH; Long et al. 2015). The major S-containing secondary metabolites exclusive to the order *Brassicales* are glucosinolates (GSLs) (Grubb and Abel 2006, Halkier and Gershenzon 2006, Sønderby et al. 2010, Ishida et al. 2014). GSLs are flavor and odor donors for *Brassica* vegetables (Bell et al. 2018). Some GSLs and their breakdown products have cancer- and cardiovascular disease-preventive effects in humans (Talalay and Fahey 2001, Traka and Mithen 2009, Ishida et al. 2014, Traka 2016). For plants, induction of GSL catabolism to produce toxic compounds or signaling molecules is an effective defense strategy against herbivory and pathogen attack (Grubb and Abel 2006, Halkier and Gershenzon 2006, Bednarek et al. 2009, Clay et al. 2009, Wittstock and Burow 2010). These noteworthy physiological functions of GSLs have encouraged studies on their metabolism.

A characteristic feature of the GSL structure is a core sulfated isothiocyanate (ITC) group conjugated with thioglucose and an R-group derived from amino acids (Clarke 2010). Depending on the amino acid precursor, GSLs can be divided into three groups: aliphatic, indolic and aromatic GSLs (Grubb and Abel 2006, Halkier and Gershenzon 2006). In *Arabidopsis thaliana*, around 40 structurally diverse GSLs are found, which are mainly methionine-derived aliphatic GSLs (mGSL) and tryptophan-derived indolic GSLs (iGSL) (Brown et al. 2003, Halkier and Gershenzon 2006). Depending on the structures, mGSL can be further classified into methylsulfanylalkyl GSLs (MSOX), such as 3MSOP, 4MSOB, 7MSOH, and 8MSOO, and methylthioalkyl GSLs (MTX), such as 4MTB, 7MTH, and 8MTO (Grubb and Abel 2006, Halkier and Gershenzon 2006, Sønderby et al. 2010, Ishida et al. 2014). mGSLs are dominant in rosette leaves, whereas iGSLs are higher in roots (Petersen et al. 2002, Brown et al. 2003). Among mGSL species, 4MSOB, 3MSOP, 4MTB, and 8MSOO are the major mGSLs, while indol-3-ylmethyl GSL (I3M) is the main iGSL accumulated in

developing rosette leaves (Petersen et al. 2002, Brown et al. 2003, Maruyama-Nakashita et al. 2006). The organ-specific GSL distribution is the result of coordination among GSL biosynthesis and catabolism, as well as the long-distance transport facilitated by GSL Transporter1 (GTR1) and GTR2 (Andersen et al. 2013).

GSLs make up 10–30% of organic S in *Brassica* plants, and their content is influenced by S availability. S fertilization led to increased GSL content in *Brassica* crops (Falk et al. 2007). S deficiency (–S) caused drastic reduction in both mGSL and iGSL in *Arabidopsis* (Maruyama-Nakashita et al. 2006, Aarabi et al. 2016). These phenomena indicated that GSLs have S storage function. Indeed, the double disruption mutants of *GTR1* and *GTR2* failed to accumulate GSLs in seeds, which therefore could not grow well under –S (Nour-Eldin et al. 2012). Under –S, plants optimize S utilization by stimulating sulfate uptake, S assimilation, and the degradation of GSH and GSLs, with the simultaneous repression of GSL biosynthesis, which is coordinated by a central transcriptional regulator of –S responses in *Arabidopsis*, SULFUR LIMITATION 1 (SLIM1) (Maruyama-Nakashita et al. 2006, Maruyama-Nakashita 2017). The repression of mGSL biosynthesis under –S is facilitated by *Sulfur Deficiency Induced (SDI) 1* and *SDI2* by repressing the transactivation activity of MYB28, a positive regulator for mGSL biosynthesis (Gigolashvili et al. 2007, Hirai et al. 2007), which leads to the downregulation of mGSL synthetic genes, such as *BCAT4*, *MAM1* and *CYP79F2* (Aarabi et al. 2016). Although the disruption of both *SDI1* and *SDI2* attenuated the decrease in mGSL levels under –S, it did not result in the recovery of mGSL levels to those under S sufficiency (+S; Aarabi et al. 2016), indicating the role of GSL catabolism in completing the impairment of GSL accumulation under –S.

To understand the molecular mechanism and physiological significance of altered GSL metabolism under –S, more insights about –S-induced GSL catabolism are required. GSLs are known to be hydrolyzed by a group of β -glucosidases (BGLUs) termed as myrosinases (Xu et al. 2004, Wittstock and Burow 2010, Nakano et al. 2017). In intact plant tissues, GSLs and myrosinases are accumulated separately in either different cells or different subcellular compartments but mix with each other upon plant cell collapse, which leads to the sudden hydrolysis of GSLs, the so-called ‘mustard oil bomb’ (Wittstock and Burow 2010, Koroleva and Cramer 2011, Chhajed et al. 2019). Upon GSL hydrolysis, glucose and sulfate are released and then a remaining intermediate is converted into ITC, simple nitrile, or epithionitrile depending on the existence of epithiospecifier modifier protein (ESM), nitrile specifier protein (NSP), or epithiospecifier protein (ESP), respectively (Zhang et al. 2006, Burow and Wittstock 2009, Wittstock and Burow 2010, Wittstock et al. 2016, Hanschen et al. 2018). There are 47 *BGLU* genes and one *BGLU*-like gene in the *Arabidopsis* genome (Xu et al. 2004), and 22 of these are suggested to encode myrosinases (Nakano et al. 2017). Depending on the specific GSL-binding signatures on their amino acid sequences, these 22 BGLUs can be further classified into two classes, atypical myrosinases, *BGLU18*–*BGLU33*, and classic myrosinases, *BGLU34*–*BGLU39* (TGG1–TGG6) (Nakano et al. 2017). Classic myrosinases, such as TGG1 and TGG2, with their wide

substrate specificities have been recognized for some time (Zhou et al. 2012). Atypical myrosinases, such as *PEN2/BGLU26* and *PYK10/BGLU23*, were identified more recently with narrower substrate specificities partial to iGSL (Bednarek et al. 2009, Nakano et al. 2017).

The –S-induced expression of two putative atypical myrosinase genes, *BGLU28* and *BGLU30*, has implied their roles in GSL catabolism under –S (Maruyama-Nakashita et al. 2003, Nikiforova et al. 2003, Hirai et al. 2004, Maruyama-Nakashita et al. 2006, Maruyama-Nakashita 2017). To clarify the contribution of these two myrosinases to –S-induced GSL catabolism and the physiological significance of this catabolic process in plant adaptation to –S, we analyzed the accumulation of GSLs and other S compounds and the expression of –S-responsive genes in the single and double disruption lines of *BGLU28* and *BGLU30*, *bglu28*, *bglu30*, and *bglu28/30*, respectively. Growth retardation in the *bglu28/30* mutants indicated the requirement of GSL catabolism to sustain plant growth under –S. These findings improve our understanding of plant adaptation to the –S environment and contribute to improving the production of health beneficial natural products in *Brassica* crops.

Results

BGLU28* and *BGLU30* are sulfur deficiency (–S)-inducible putative *BGLU* genes regulated by *SLIM1

Two putative *BGLU* genes, *BGLU28* and *BGLU30*, have been known for their inducibilities under –S (Maruyama-Nakashita et al. 2003, Nikiforova et al. 2003, Hirai et al. 2004, Maruyama-Nakashita et al. 2006; Fig. 1A). Transcript levels of both *BGLU28* and *BGLU30* were upregulated upon short- and long-term –S treatments with higher and earlier responses in *BGLU28* (Fig. 1A; Maruyama-Nakashita et al. 2005, 2006). The upregulations were moderated in *slim1* mutants (Fig. 1A; Maruyama-Nakashita et al. 2006), indicating that –S-induced expression of *BGLU28* and *BGLU30* was regulated by *SLIM1*. According to the phylogenetic analysis of myrosinase family genes, atypical and classic myrosinases were separated. Atypical myrosinases can be further classified into three different clades, *BGLU33*, *BGLU28* to *BGLU32*, and *BGLU18* to *BGLU27* to which *PEN2/BGLU26* and *PYK10/BGLU23* belonged (Fig. 1B; Nakano et al. 2017). Among *BGLU28* to *BGLU32*, *BGLU28* to *BGLU30* maintained higher similarity sharing 65.5–72.5% identity with each other, indicating their similar functions in plants (Fig. 1B). Unlike *BGLU28* and *BGLU30*, the transcript level of *BGLU29* was neither detected nor upregulated by –S in the previous transcriptome analysis (Maruyama-Nakashita et al. 2003, Nikiforova et al. 2003, Hirai et al. 2004, Maruyama-Nakashita et al. 2006, Aarabi et al. 2016). Therefore, we decided to clarify the physiological functions of *BGLU28* and *BGLU30* under –S.

GSL content was higher in the double disruption line of *BGLU28* and *BGLU30* than in wild-type plants under –S

To investigate whether *BGLU28* and *BGLU30* are responsible for –S-induced GSL catabolism, we isolated the single and

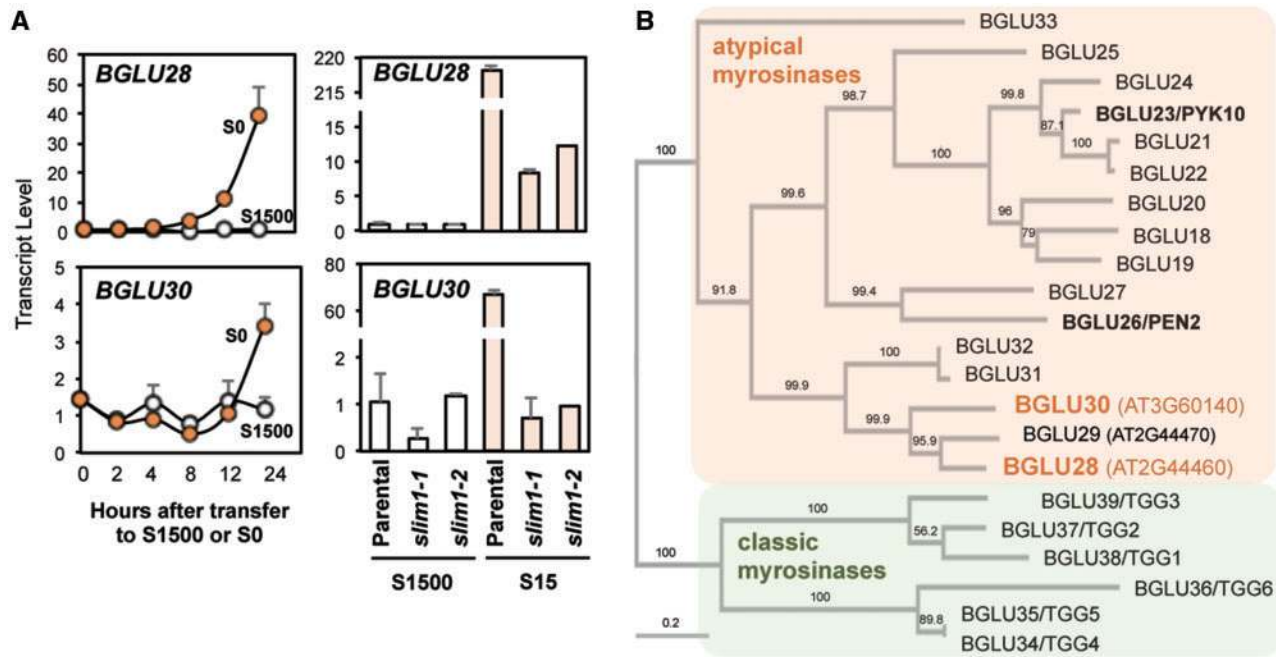


Fig. 1 BGLU28 and BGLU30 in *Arabidopsis*. (A) Transcript levels of BGLU28 and BGLU30 in roots of 10-day-old WT plants transferred from the agar media supplied with 1,500 μM (S sufficient, S1500) to S1500 (white) or to the agar media without sulfate (no sulfate, S0; orange) (left, Maruyama-Nakashita et al. 2005) and those in the roots of 10-day-old *slim1-1*, *slim1-2*, and the parental plants grown on S1500 (white) and the agar media supplied with 15 μM (S deficient, S15, light orange) sulfate (right, Maruyama-Nakashita et al. 2006). The values and error bars indicate mean \pm SEM ($n = 2$). (B) Phylogenetic relationships of BGLUs classified as myrosinases in *Arabidopsis*. Protein sequences obtained from the National Center for Biotechnology Information (<https://www.ncbi.nlm.nih.gov/>) were aligned with ClustalW, and the phylogenetic tree was drawn using ETE3 (<https://www.genome.jp/tools-bin/clustalw>).

double disruption lines of BGLU28 and BGLU30, *bglu28*, *bglu30*, and *bglu28/30*, respectively, using PCR-based selections (Sessions et al. 2002, Alonso et al. 2003; Supplementary Table S1, Supplementary Fig. S1) and analyzed GSL content in these disruption lines and wild-type (WT) plants (Fig. 2). Plants were grown for 10 d on agar medium supplemented with sufficient (1500 μM , S1500), deficient (15 μM , S15) or no (0 μM , S0) sulfate. Under S1500, GSL content (nmol per plant) in *bglu* lines was similar to that in WT plants. In contrast, except for undetectable I3M level under S0 (Supplementary Table S3), the content of MTX, MSOX, and I3M was much higher in the *bglu28/30* mutants than that in *bglu28*, *bglu30*, and WT plants under S15 and S0 (Fig. 2). GSL concentrations [nmol/mg fresh weight (mg FW)] were also increased in *bglu28/30* mutants compared to those in *bglu28*, *bglu30*, and WT plants under S15 and S0 (Supplementary Fig. S2). These results supported the hypothesis that BGLU28 and BGLU30 catalyze GSL hydrolysis upon $-S$.

Growth retardation of *bglu28/30* mutants under $-S$

In addition to higher GSL accumulation under $-S$, growth was strongly reduced in *bglu28/30* mutants under $-S$ (Fig. 3A). Root length and FW of *bglu28/30* and *bglu28* mutants were significantly decreased compared to those of WT plants under the same S conditions except for the FW of *bglu28* mutants under S1500 (Fig. 3B, C). The root length of the *bglu30* mutants was only reduced under S15, while the FW of *bglu30* mutants was similar to that of WT plants regardless of S conditions (Fig. 3B,

C). Under S0 conditions, the growth retardation in *bglu28/30* mutants was particularly noticeable, i.e. the root length was 36.6% and the FW was 36.3% that of the WT plants (Fig. 3B, C).

Disruption of BGLU28 and BGLU30 affected primary S metabolism under $-S$

Based on the retarded growth and the overaccumulation of GSL in *bglu28/30* mutants under $-S$, we assumed that primary S metabolism was affected by the decrease in sulfate supply from GSL catabolism. To confirm this hypothesis, we analyzed the levels of total S, GSH, cysteine, and sulfate accumulated in *bglu* mutants and WT plants under different S conditions (Fig. 4). Total S content (nmol per plant) in *bglu* mutants and WT plants was similar under all S conditions (Fig. 4). GSH and cysteine content was similar among the plant lines under S1500 and S15; however, under S0, GSH content tended to be decreased in *bglu28/30* mutants and cysteine content was significantly reduced in *bglu28/30* mutants compared to that in WT plants (Fig. 4). Sulfate content in *bglu* mutants was lower than that in WT plants under S15 (Fig. 4). Under S0, sulfate level was below the detection limit in all genotypes (data not shown). Taken together, loss of sulfate released from GSL catabolism would have an impact on the accumulation of GSH, cysteine, and sulfate under $-S$. Concentrations of total S, GSH, cysteine, and sulfate (nmol/mg FW) were almost similar among plant lines, except for the increase in cysteine in *bglu30* and *bglu28/30* mutants under S15 and the increase in total S in *bglu28/30*

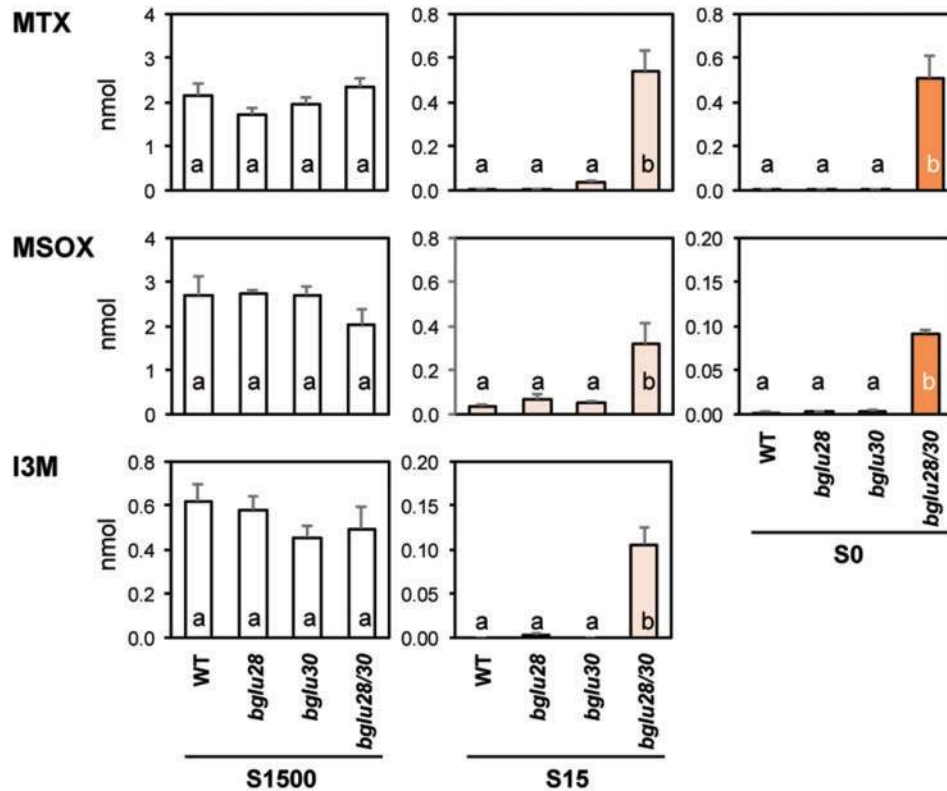


Fig. 2 GSL content in *bglu* mutants and WT plants grown under different sulfur (S) conditions. Plants were vertically grown for 10 d on the agar media supplied with sufficient (1,500 μ M, S1500, white), deficient (15 μ M, S15, light orange), or no (0 μ M, S0, orange) sulfate. GSLs were analyzed using liquid chromatography–mass spectrometry (LC–MS), and the content (nmol) per plant was calculated following the standard curve. The values and error bars indicate mean \pm SEM ($n = 4$). One-way analysis of variance (ANOVA) followed by the Tukey–Kramer test was applied to the four genotypes grown under the same conditions. Different letters indicate significant differences ($P < 0.05$).

mutants under S0 compared to that in WT plants under the same S conditions (Supplementary Fig. S3).

Disruption of *BGLU28* and *BGLU30* caused decrease in protein content and S content in protein under $-S$

Cysteine and methionine, S-containing amino acids produced by the S assimilatory pathway, are mainly used for protein synthesis. As cysteine content was reduced in *bglu28/30* mutants under S0, protein level and S incorporation into protein could also be decreased in *bglu28/30* mutants under $-S$. To test this possibility, we analyzed protein content and S content in protein fractions of *bglu28/30* and WT plants grown under different S conditions (Fig. 5).

Protein levels were analyzed with a colorimetric assay (Bradford 1976; Fig. 5). Compared with WT plants under the same S conditions, protein content (μ g per plant) in *bglu28/30* mutants was decreased in general (Fig. 5). Protein concentrations (nmol/mg FW) in *bglu28/30* mutants were decreased under S1500 and S15, whereas they were similar under S0 compared to that in WT plants (Supplementary Fig. S4).

S content in the protein fraction was analyzed as the total S content in the precipitated fraction with 80% ethanol together with that in the soluble fraction (Christianson et al. 1965a, Christianson et al. 1965b; Fig. 5). S content in the protein

fraction (nmol per plant) of *bglu28/30* mutants was lowered under S0 compared with that of WT plants, while it was similar with that of WT under S15 and S1500 (Fig. 5). In contrast, S content in the soluble fraction (nmol per plant) of *bglu28/30* mutants was higher than that of WT plants under S15 and S0 (Fig. 5), which probably owing to the higher accumulation of GSL (Fig. 2). S concentrations (nmol per mg FW) in both the soluble and protein fractions of *bglu28/30* mutants were increased under S15 and S0 (Supplementary Fig. S4).

$-S$ responses were enhanced in *bglu28/30* mutants

To investigate the influence of impaired GSL catabolism under $-S$ on S metabolism, we compared the transcript levels of several $-S$ -responsive genes in *bglu28/30* mutants with those in WT plants. *SULTR1;2* is the main contributor for sulfate uptake, and *SULTR4;2* facilitates the retrieval of stored sulfate from vacuoles (Takahashi et al. 2011, Long et al. 2015). *APR2* and *APR3* encode 5'-adenylylsulfate (APS) reductase, which catalyzes the reduction in APS to sulfite (Long et al. 2015). *GGCT2;1* is responsible for GSH degradation under $-S$ (Paulose et al. 2013). *BCAT4* and *MAM1* play roles in the side chain elongation, and *CYP79F2* is involved in the core structure formation of mGSL (Grubb and Abel 2006, Halkier and Gershenzon 2006, Sønderby et al. 2010). *GTR1* encodes a high-affinity GSL transporter (Nour-Eldin et al.

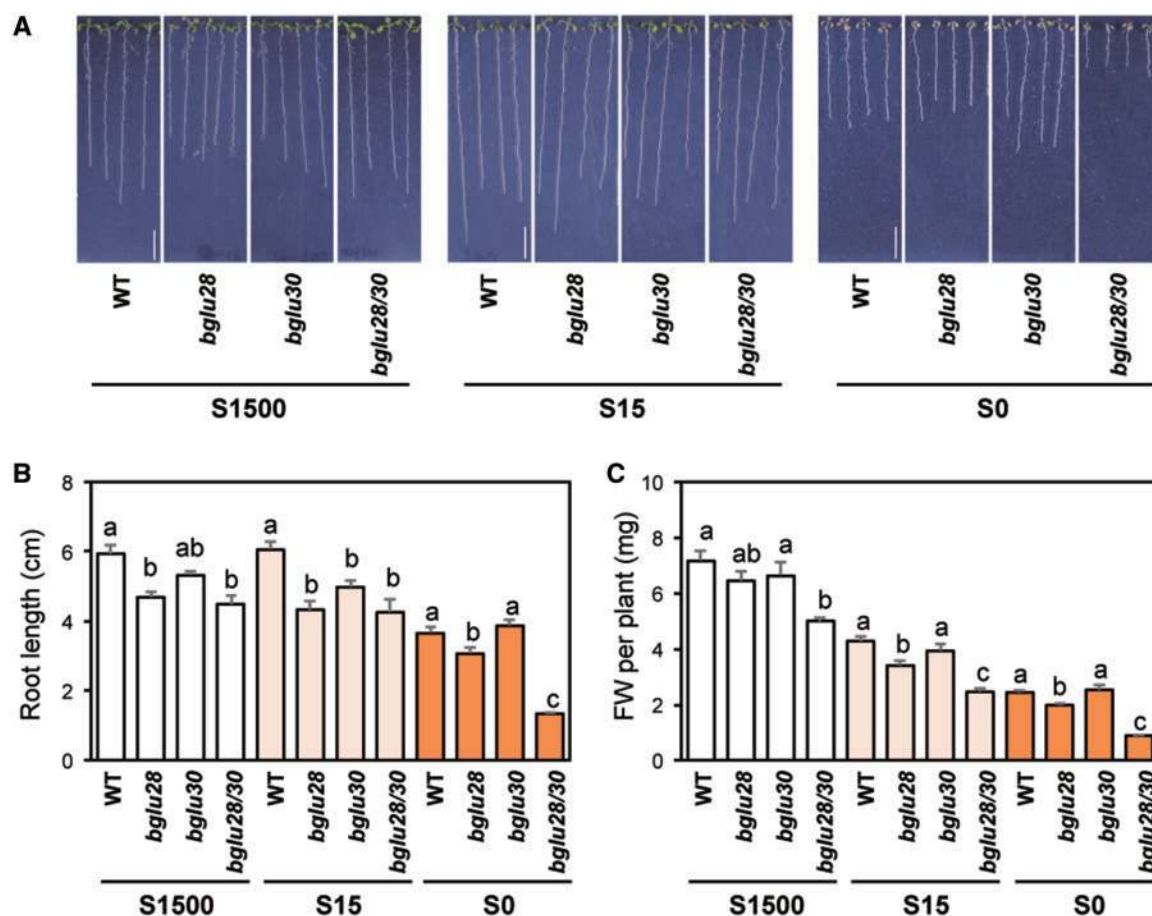


Fig. 3 Growth phenotypes of *bglu* mutants and WT plants grown under different S conditions. (A) Representative images of plants grown on the media. Scale bar, 1 cm. (B) Root lengths ($n = 8$). (C) FW per plant ($n = 4$). Plants were vertically grown for 8 d on S1500 (white), S15 (light orange), or S0 (orange) agar media. The values and error bars indicate mean \pm SEM. One-way ANOVA followed by the Tukey–Kramer test was applied to the four genotypes grown under the same conditions. Different letters indicate significant differences ($P < 0.05$).

2012). SDI1 transcriptionally inhibits GSL biosynthesis upon $-S$ (Aarabi et al. 2016).

When S was limited, transcript levels of *BCAT4*, *MAM1*, and *CYP79F2* were downregulated, while those of the others were upregulated in WT plants (Fig. 6), which was consistent with results mentioned in a previous reports (Maruyama-Nakashita 2017). In the *bglu28/30* mutants, the expression levels of these $-S$ -responsive genes were similarly regulated by $-S$ as those in WT plants. Notably, transcript levels of *SULTR1;2* were higher in *bglu28/30* mutants than those in WT plants under $-S$. The transcript levels of other $-S$ -upregulated genes, especially *APR2* and *GTR1*, also tended to be higher in *bglu28/30* mutants relative to those in WT plants under $-S$ (Fig. 6). From this analysis, *bglu28/30* mutants responded to $-S$ to a greater extent than that in WT plants, suggesting that plants enhanced sulfate acquisition from the environment when the supply of sulfate from GSL catabolism was blocked under $-S$.

Discussion

BGLU28 and BGLU30 have been suggested as responsible for $-S$ -induced GSL catabolism for over 15 years (Maruyama-Nakashita et al. 2003, 2005, 2006, Nikiforova

et al. 2003, Hirai et al. 2004), albeit their physiological functions under $-S$ were barely investigated. The $-S$ -induced expression of *BGLU28* and *BGLU30* were eliminated in *slim1* mutants, which accompanied the abundant accumulation of GSLs under $-S$ (Maruyama-Nakashita et al. 2006). Consistent with the previous suggestions, we found that dysfunction of both *BGLU28* and *BGLU30* led to overaccumulation of GSLs under $-S$ (Fig. 2; Supplementary Fig. S2). Similar GSL levels in both *bglu28* and *bglu30* mutants to that in WT plants without enhancing the expression of the other one (Supplementary Fig. S5) suggested that myrosinase activity of either BGLU28 or BGLU30 is strong enough to compensate for the loss of the other. As the similar repression of mGSL biosynthetic gene expressions by $-S$ was observed between *bglu28/30* and WT plants (Fig. 6), the possibility of enhanced mGSL biosynthesis in *bglu28/30* mutants was excluded. Taken together, our findings indicated myrosinase activity of BGLU28 and BGLU30 under $-S$ in planta. As there is no report to demonstrate their enzymatic activities in vivo nor in vitro, this is the first report for their function as myrosinases.

Atypical myrosinases are presumed to catalyze the hydrolysis of specific GSLs under particular biotic or abiotic stresses

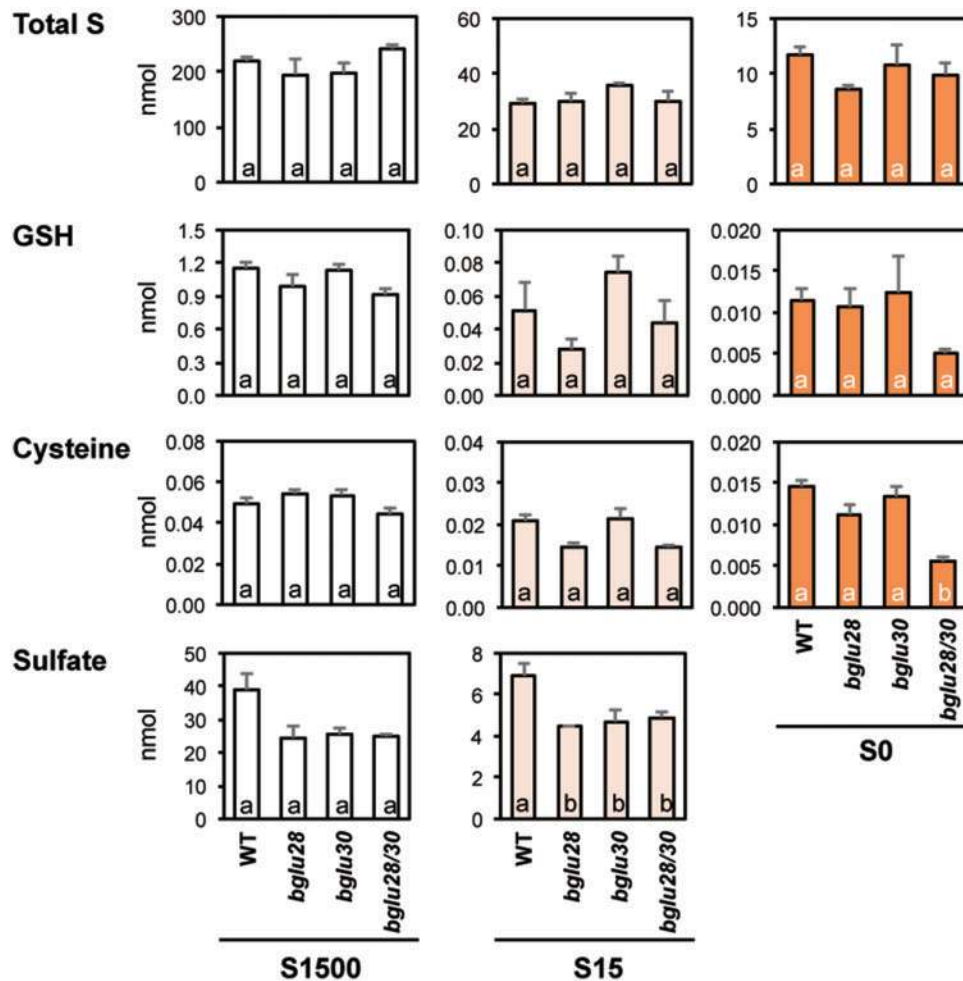


Fig. 4 Total S, GSH, cysteine, and sulfate contents in WT plants and *bglu* mutants grown under different S conditions. Plants were vertically grown for 10 d on S1500 (white), S15 (light orange), and S0 (orange) agar media. Total S, GSH and cysteine, and sulfate were analyzed using ICP-MS, HPLC-fluorescent system, and ion chromatography, respectively, and the content (nmol) per plant was calculated. The values and error bars indicate mean \pm SEM ($n = 4$). One-way ANOVA followed by the Tukey–Kramer test was applied to the four genotypes grown under the same conditions. Different letters indicate significant differences ($P < 0.05$).

(Bednarek *et al.* 2009, Clay *et al.* 2009, Nakano *et al.* 2017). For example, PEN2/BGLU26 and PYK10/BGLU23 were reported to hydrolyze an iGSL, 4-methoxyindol-3-ylmethylglucosinolate (4MI3G), upon pathogen or herbivore attack (Bednarek *et al.* 2009, Nakano *et al.* 2017). Although both mGSL and iGSL levels were higher in *bglu28/30* mutants than those in WT under S15, we could not detect I3M under more severe $-S$ condition, S0, which suggested the contribution of the other BGLU to hydrolyze I3M or the repression of I3M distribution to the shoot under S0. Comparing the two structurally diverse mGSLs, MTX and MSOX, the decrease in MTX in WT plants under $-S$ was more drastic than that of MSOX as well as the ratio of their levels between *bglu28/30* and WT plants (Supplementary Tables S3, S4). These results suggest that MTX are preferred substrates for BGLU28 and BGLU30 under $-S$ relative to MSOX. Among MTX species, 4MTB, 7MTH, and 8MTO, the ratio of 4MTB between *bglu28/30* and WT plants was higher than that of the others under both S15 and S0 conditions, while their ratios between S15–S1500 and S0–S1500 were not much different (Supplementary Tables S3, S4). It is plausible that 4MTB

is preferentially hydrolyzed by BGLU28 and BGLU30 upon $-S$, and along with the severity of $-S$, hydrolysis of 7MTH and 8MTO is initiated by them. Precise characterization of the biochemical properties of BGLU28 and BGLU30 is required to determine their substrate specificities.

Although it is known that GSL catabolism was induced by $-S$, how this hydrolysis happens in intact tissues remains a question to be clarified. GSLs are reported to be stored in the vacuole (Grob and Matile 1979, Matile 1980). BGLU28 and BGLU30 are also predicted to be localized in the vacuole (SUBA3, <http://suba3.plantenergy.uwa.edu.au/>; Tanz *et al.* 2013, Hooper *et al.* 2014). Once the expression of BGLU28 and BGLU30 is induced by $-S$, their proteins can appear in the vacuole where they can hydrolyze the stored GSLs. Then, the sulfate released in the vacuole can be exported to the cytosol through the function of SULTR4;1 and SULTR4;2, the expressions of which are also increased under $-S$, further enabling the recycling of S for S assimilation (Kataoka *et al.* 2004). BGLU30 is also predicted to localize in the extracellular space (SUBA4, <http://SUBA.live/>; Hooper *et al.* 2017), in which GSL hydrolysis

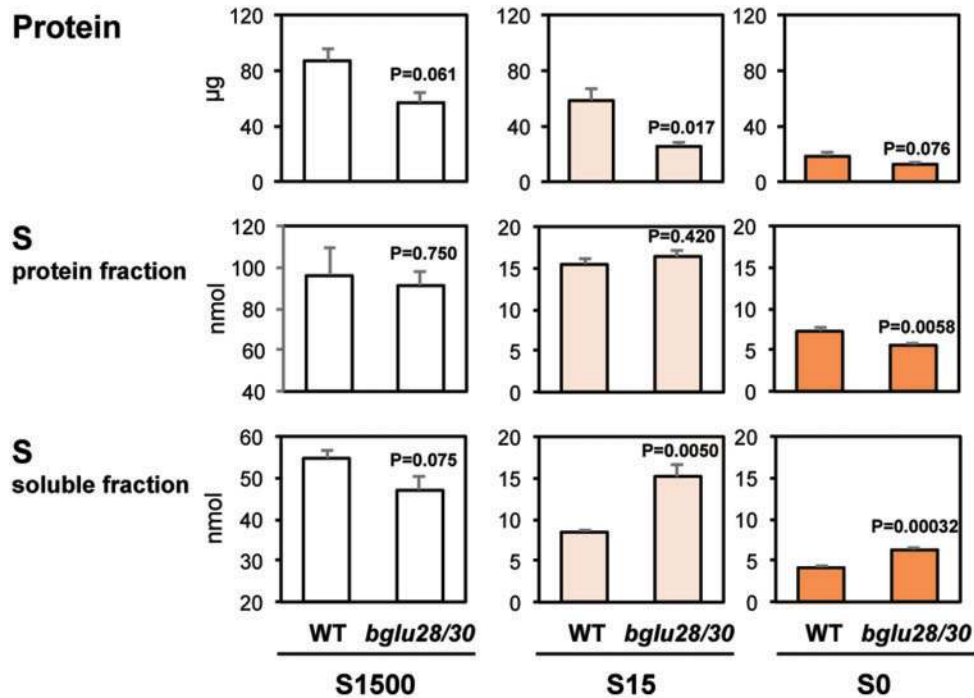


Fig. 5 Protein content and S content in protein and supernatant fraction of WT plants and *bglu28/30* mutants grown under different S conditions. Plants were vertically grown for 10 d on S1500 (white), S15 (light orange), and S0 (orange) agar media. Protein levels were analyzed colorimetrically, and the content per plant (μg , top) was calculated. Protein fractions were obtained as the precipitate with 80% ethanol. S levels in the precipitate (middle) and the supernatant (bottom) were analyzed using ICP-MS. The content per plant (nmol) was calculated based on the standard curve. The values and error bars indicate mean \pm SEM ($n = 4$). *P*-values detected with the Student's *t*-test between WT plants and *bglu28/30* mutants are presented on the bars.

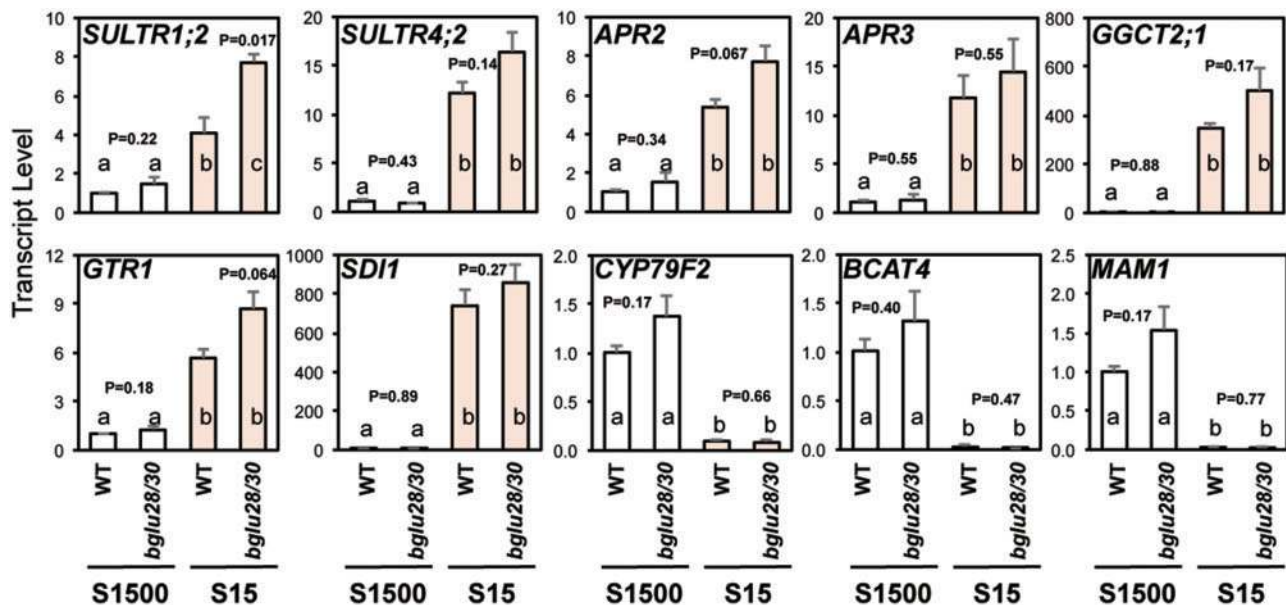


Fig. 6 Transcript levels of $-S$ -responsive genes in WT plants and *bglu28/30* mutants grown under S1500 and S15 conditions. Plants were vertically grown for 8 d on S1500 (white) and S15 (light orange) agar media. Transcript levels of $-S$ -responsive genes in roots of WT plants and *bglu28/30* mutants were analyzed using quantitative reverse transcription-polymerase chain reaction (qRT-PCR). Two-way ANOVA followed by the Tukey–Kramer test was applied to all experimental conditions. Different letters indicate significant differences ($P < 0.05$). *P*-values detected with the Student's *t*-test between WT plants and *bglu28/30* mutants are presented on the bars.

may be effective in excluding the toxic effects of ITCs in the cell. In this case, GSLs have to be transported to the extracellular space via GSL transporters, which have not yet been identified (Andersen *et al.* 2013). Considering that the optimal pH for other known myrosinases was around 5.5 (Bednarek *et al.* 2009, Zhou *et al.* 2012, Nakano *et al.* 2017), both vacuole and extracellular spaces where pH is maintained from 5.0 to 6.0 are suitable for GSL hydrolysis (Felle 2001, Shimada *et al.* 2018). Experimental data about the subcellular localizations of each GSL, BGLU28 and BGLU30, and the transport machinery of GSL inside and outside of the cells would be desirable to confirm these expectations.

After the release of glucose and sulfate moieties, the remaining parts of GSLs are further metabolized to nitriles, epithionitriles, and ITCs depending on the existence of NSP, ESP and ESM, respectively (Zhang *et al.* 2006, Burow and Wittstock 2009, Wittstock and Burow 2010, Wittstock *et al.* 2016). Interestingly, the transcript level of an NSP family gene member in *Arabidopsis*, *NSP5*, was upregulated by $-S$ (Maruyama-Nakashita *et al.* 2006). The products of NSP-dependent GSL hydrolysis, simple nitriles, are further metabolized to carboxylic acids and amide by nitrilase (NIT) activity (Janowitz *et al.* 2009, Wittstock and Burow 2010). Among the three isoforms of NITs in *Arabidopsis*, NIT1, 2, and 3, which preferably use simple nitriles as the substrates, the expression of *NIT3* was also upregulated by $-S$ (Kutz *et al.* 2002, Nikiforova *et al.* 2003). This NSP-dependent GSL catabolic pathway is assumed to have two physiological advantages with regard to S metabolism: (i) plants can avoid the production of toxic chemicals, such as ITCs, in the cell, which is beneficial for GSL catabolism without tissue disruption, and (ii) one more S-containing moiety can be liberated upon nitrile formation, which can be further utilized for primary S metabolism (Janowitz *et al.* 2009, Wittstock and Burow 2010). In addition, the S moiety in the side chain of mGSLs might be recycled to primary S metabolism, although the metabolic pathway has not been determined. Taken together, it is plausible that $-S$ stress induces NSP-dependent GSL catabolism to optimize S usage using GSLs as S storage.

Another question of interest was the role of GSL catabolism in plant growth under $-S$. The physiological significance of $-S$ -induced GSL catabolism is considered to provide sulfate for primary S metabolism (Fig. 7; Maruyama-Nakashita *et al.* 2003, Nikiforova *et al.* 2003, Hirai *et al.* 2004, Maruyama-Nakashita *et al.* 2006). Plant growth was inhibited under both S15 and S0 conditions (Fig. 3), along with a decrease in total S, the S-containing compounds analyzed, and protein levels (Figs. 2, 4, 5). In the comparison between *bglu28/30* and WT plants, the amount of S contained in GSL in *bglu28/30* mutants under S15 was 79 ng (per plant) more than that in WT plants, whereas the S contained in the other S-containing compounds, cysteine, GSH, sulfate, and S in protein fraction was lowered by only 36 ng (per plant) in *bglu28/30* mutants (Supplementary Table S5). This inconsistency might be due to the reduction in other S-containing compounds except those we analyzed. Also, loss of recycled sulfate in *bglu28/30* mutants reinforced sulfate

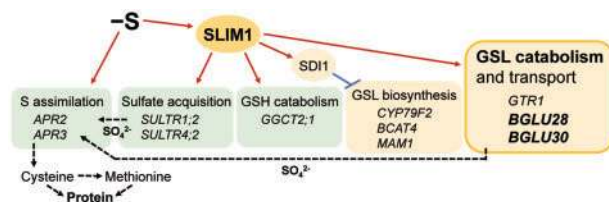


Fig. 7 Coordination of S metabolism under $-S$. Upon $-S$, S assimilation, sulfate acquisition, GSH and GSL catabolism, and GSL transport are stimulated (red arrow) and GSL synthesis is repressed (blue line). SLIM1 regulates most of these metabolic pathways under $-S$. Sulfate acquisition, S assimilation, and GSH catabolism belong to primary S metabolism (green box). GSL metabolism is defined as specific metabolism (yellow box). Flow of sulfate under $-S$ is indicated by the black-dotted arrow. Representative genes (italic) involved in each metabolic pathway are presented. *APR*, 5'-adenylylsulfate reductase; *SULTR*, sulfate transporter; *GGCT*, γ -glutamyl cyclotransferase; *CYP79*, cytochromes P450 of the CYP79 family; *BCAT*, branched-chain amino acid aminotransferase; *MAM*, methylthioalkylmalate synthase; *GTR*, glucosinolate transporter.

uptake from the environment and possibly enhanced the S assimilation process (Figs. 6, 7). Under S0, S content in the increased GSL fraction (50 ng per plant) in *bglu28/30* mutants almost equals that in the decreased fraction of the other S-containing compounds analyzed (55 ng per plant) (Supplementary Table S5). These results suggested that sulfate released from GSLs is considerable for maintaining primary S metabolism upon $-S$. In addition, the lower level of protein in *bglu28/30* mutants may be the reason for their growth retardation regardless of the S conditions, and under severe $-S$ condition (S0), the lower level of S content in the protein fraction of *bglu28/30* mutants may make the growth retardation more obvious (Figs. 3, 5).

Of course, other possibilities are still open to explain the observed growth retardation in *bglu28/30* mutants, e.g. higher accumulation of GSL under $-S$ itself can inhibit plant growth, or the metabolites derived by GSL hydrolysis could be required for plant growth. GSLs or their breakdown products may serve as signaling molecules interacting with other pathways to mediate plant growth. For instance, myrosinase-dependent mGSL catabolism was reported to perform signaling function in promoting stomatal closure and thus regulate plant growth under drought stress (Salehin *et al.* 2019). 3-Hydroxy-propyl-glucosinolate was able to regulate root development via interaction with the Target of Rapamycin (TOR) signaling pathway (Malinovsky *et al.* 2017). An iGSL breakdown product, indole-3-carbinol, was reported to act as a signaling molecule and competes with TIR1-dependent auxin signaling to alter plant growth (Katz *et al.* 2015). Further investigation is required to determine whether GSL metabolism mediated by BGLU28 and BGLU30 has signaling function under $-S$.

In summary, the findings in this study proved that BGLU28 and BGLU30 are responsible for $-S$ -induced GSL catabolism and activating S storage function of GSLs (Fig. 2; Supplementary Fig. S2, Tables S3, S4). A decrease in S-containing metabolites in *bglu28/30* mutants suggested that GSL

hydrolysis is important to maintain primary S metabolism necessary for plant growth under $-S$ (Fig. 4; Supplementary Fig. S3). The knowledge obtained here deepens our understanding of plant adaptation strategies to $-S$ environments (Fig. 7) and thus provides implications for promoting effective S utilization in modern agriculture. Characterization of key enzymes that regulate GSL metabolism shed light on designing strategies to manipulate the accumulation of these specific metabolites beneficial to health in *Brassica* crops.

Materials and Methods

Plant materials and growth conditions

The *A. thaliana* ecotype, Columbia (Col-0), was used as the WT. The T-DNA insertion mutants of *BGLU28* (At2g44460, SALK_043339) and *BGLU30* (At3g60140, SAIL_694_G08) were obtained from the Arabidopsis Biological Resource Center (ABRC). Confirmation of T-DNA insertions and homozygous insertions in these mutants were carried out by PCR-based screening using T-DNA left border primers and gene-specific primers for *BGLU28* and *BGLU30* (Sessions et al. 2002, Alonso et al. 2003; Supplementary Table S1). The resultant homozygous mutants carrying T-DNA insertion in the fourth exon of *BGLU28* and the eighth exon of *BGLU30* were named as *bglu28* and *bglu30*, respectively (Supplementary Fig. S1A). Double disruption line of *BGLU28* and *BGLU30* was generated by cross-fertilization of *bglu28* and *bglu30* and the following PCR-based screening in *F2* progenies. *F3* progenies without *BGLU28* and *BGLU30* expression were named as *bglu28/30*. Disruption of transcripts by T-DNA insertions was confirmed using RT-PCR (Supplementary Table S1, Fig. S1B).

Plants were vertically grown on mineral nutrient media (Fujiwara et al. 1992, Hirai et al. 1995) containing 1% sucrose and 0.8% agarose, at 22°C under constant illumination (40 $\mu\text{mol}/\text{m}^2/\text{s}^{-1}$). Agar medium was prepared as described previously (Kimura et al. 2019). S1500 agar medium was supplemented with 1,500 μM MgSO_4 . S15 agar medium was supplemented with 15 μM MgSO_4 , and Mg concentration was adjusted to 1,500 μM with MgCl_2 . S0 agar medium was supplemented with 1,500 μM MgCl_2 . Ten days after sowing the seeds, plants were harvested, rinsed with distilled water, frozen in liquid nitrogen, and stored at -80°C until further analysis. Just before the metabolite and transcript analysis, the plant samples were ground into fine powder using Tissue Lyser MM300 (Retsch, Düsseldorf, Germany).

Measurements of GSLs

Metabolites were extracted with 300 μl of ice-cold 80% methanol containing 2 μM (+)-10-camphor sulfonic acid (10CS, internal standard for negative ionization mode; Tokyo Kasei, Japan). After homogenization, cell debris was removed by centrifugation (14,000 rpm, 10 min, 4°C) and the supernatants were vacuum evaporated. Dried supernatants were dissolved into 100 μl ultra-pure water and filtrated with Millex-GV filter units (Millipore, USA) prior to the analysis.

GSL levels were analyzed using a high-performance liquid chromatograph connected to a triple quadrupole-MS (LCMS-8050; Shimadzu, Kyoto, Japan) using L-column 2 ODS (pore size 3 μm , 2.1 mm \times 150 mm; CERI, Japan) as described previously (Matsuda et al. 2009, Morikawa-Ichinose et al. 2019). The mobile phases were as follows: A, ultra-pure water with 0.1% formic acid; B, acetonitrile with 0.1% formic acid. The gradient program was as follows with a flow rate of 0.3 ml/min: 0–0.1 min, 1% B; 0.1–15.5 min, 1–99.5% B; 15.5–17 min, 99.5% B; 17.1–20 min, 1% B. The mass spectrometer was run in negative electrospray mode. GSLs levels were quantified with calibration curve using standard GSL compounds (4MTB, 3MSOP, 4MSOB, I3M; Cfm Oskar Tropitzsch GmbH, Marktredwitz, Germany).

Observation of plant phenotype

Plants were vertically grown for 8 d. The root lengths of plants were measured using scales, and the plant images were captured using a STAGE-2000-BG system (AMZ System Science, Japan).

Measurement of total S

Plant samples were digested in 200 μl of conc. HNO_3 (Nacalai Tesque, Kyoto, Japan) at 95°C for 30 min followed by an incubation at 115°C for 90 min. After confirming complete digestion, the samples were cooled to room temperature, diluted to 1 ml with ultra-pure water and filtrated with 0.45- μm filters (DISMIC-03CP; ADVANTEC, Japan). The processed samples were diluted 10-fold in 0.1 M HNO_3 containing gallium (KANTO CHEMICAL, Tokyo, Japan) as an internal standard immediately before the analysis. S levels were analyzed using inductively coupled plasma mass spectroscopy (ICP-MS; Agilent7700x; Agilent Technologies, CA, USA) and quantified based on the standard curve derived from the analysis of an S standard solution (KANTO CHEMICAL).

Measurements of cysteine, GSH, and sulfate

The plant extracts used for GSL analysis were used for the analysis of cysteine, GSH, and sulfate. Cysteine and GSH levels were determined by HPLC-fluorescent detection system (JASCO, Tokyo, Japan) after labeling of thiol bases with monobromobimane (Invitrogen, USA) as described previously (Kimura et al. 2019). The labeled products were separated by HPLC using the TSKgel ODS-120T column (150 mm \times 4.6 mm; TOSOH, Tokyo, Japan) and detected with a fluorescence detector FP-920 (JASCO), monitoring the fluorescence at 478 nm under the excitation at 390 nm. Cysteine and GSH (Nacalai Tesque) were used as standards.

Sulfate level was determined by ion chromatograph (IC-2001; TOSOH) using a TSK SuperIC-AZ column (TOSOH) at a flow rate of 0.8 ml/min with an eluent containing 1.9 mM NaHCO_3 (Wako Pure Chemicals, Osaka, Japan) and 3.2 mM Na_2CO_3 (Wako Pure Chemicals) as described previously (Yamaguchi et al. 2016, Kimura et al. 2019). An anion mixture standard solution 1 (Wako Pure Chemicals) was used as a standard.

Measurement of total protein

Total protein was extracted with 200 μl of 5-fold diluted Cell Culture Lysis 5 \times Reagent (Promega Corporation, Madison, WI, USA). Cell debris was removed by centrifugation (10,000 rpm, 10 min, 4°C). Total protein level was determined using a Bio-Rad protein assay kit (Bradford 1976; Bio-Rad Laboratories, Inc., CA, USA) with bovine serum albumin as a standard. The color development was detected using a multimode reader with a 595-nm filter (TriStar² LB942-LA; Berthold Technologies).

Measurement of S in protein and supernatant fraction

Protein fractions were obtained through precipitation with 80% ethanol. Plant samples were homogenized with 300 μl of 80% ethanol and placed under 4°C for 24 h. Then, the precipitated proteins were collected by centrifugation (10,000 rpm, 10 min, 4°C). The supernatants were transferred to a new tube, and the same process was performed once more for the precipitates. Supernatants from the two extractions were collected in the same tube and were evaporated. Dried supernatants and precipitated proteins were digested, analyzed using ICP-MS, and quantified as described in the Measurement of total S.

Quantitative RT-PCR

RNA extraction and reverse transcription were conducted using Sepasol-RNA I (Nacalai Tesque) and PrimeScript RT Reagent Kit with gDNA Eraser (Takara, Osaka, Japan) as described previously (Kimura et al. 2019). Real-time PCR was carried out using a KAPA SYBR FAST qPCR Master Mix 2x (Kapa Biosystems, USA), a qTOWER³ G touch (Analytik Jena AG, Germany), and gene-specific primers listed in Supplementary Table S2. Primer efficiency of each primer set was assessed before the experiment. The relative mRNA abundances were calculated with $\Delta\Delta\text{Ct}$ methods using *UBQ2* as an internal control.

Statistical analysis

One-way ANOVA followed by the Tukey–Kramer test and the Student's *t*-test were performed using Microsoft Excel program installed with PHStat add-in (downloaded from <http://wps.pearsoned.com/phstat/>). Significant

differences detected by the Tukey–Kramer test are shown with different letters ($P < 0.05$), and those detected by the Student's *t*-test are shown with asterisks ($*0.01 < P < 0.05$, $**P < 0.01$) or *P*-values.

Supplementary Data

Supplementary data are available at PCP online.

Funding

Japan Society for the Promotion of Science (JSPS) Grants-in-Aid for Scientific Research (JP20770044 and JP17H03785 to A.M.-N.); Grant-in-Aid for JSPS fellow (JP16J40073 to T.M.-I.); Japan Foundation for Applied Enzymology to A.M.-N.

Acknowledgments

We gratefully acknowledge the ABRC for providing the T-DNA insertion lines of *BGLU28* and *BGLU30*. The ICP-MS (Agilent7700x) and LCMS-8050 analysis were performed at the Center of Advanced Instrumental Analysis, Kyushu University, and the Center of Advanced Instrumental and Educational Supports, Faculty of Agriculture, Kyushu University, with the kind instruction by Dr. Midori Watanabe, Dr. Yuki Mori, and Taiki Akasaka. Plant growth and seed harvesting were done at Biotron Application Center, Kyushu University. We thank Yukiko Okuo and Tsukasa Ushiwatari for technical support.

Disclosures

The authors have no conflict of interest to declare.

References

- Aarabi, F., Kusajima, M., Tohge, T., Konishi, T., Gigolashvili, T., Takamune, M., et al. (2016) Sulfur deficiency-induced repressor proteins optimize glucosinolate biosynthesis in plants. *Sci. Adv.* 2: e1601087.
- Alonso, J.M., Stepanova, A.N., Leisse, T.J., Kim, C.J., Chen, H., Shinn, P., et al. (2003) Genome-wide insertional mutagenesis of *Arabidopsis thaliana*. *Science* 301: 653–657.
- Andersen, T.G., Nour-Eldin, H.H., Fuller, V.L., Olsen, C.E., Burow, M. and Halkier, B.A. (2013) Integration of biosynthesis and long-distance transport establish organ-specific glucosinolate profiles in Vegetative *Arabidopsis*. *Plant Cell* 25: 3133–3145.
- Bednarek, P., Pislewska-Bednarek, M., Svatos, A., Schneider, B., Doubek, J., Mansurova, M., et al. (2009) A glucosinolate metabolism pathway in living plant cells mediates broad-spectrum antifungal defense. *Science* 323: 101–106.
- Bell, L., Oloyede, O.O., Lignou, S., Wagstaff, C. and Methven, L. (2018) Taste and flavor perceptions of glucosinolates, isothiocyanates, and related compounds. *Mol. Nutr. Food Res.* 62: 1700990.
- Bradford, M.M. (1976) A rapid and sensitive method for the quantitation of microgram quantities of protein utilizing the principle of protein-dye binding. *Anal. Biochem.* 72: 248–254.
- Brown, P.D., Tokuhisa, J.G., Reichelt, M. and Gershenzon, J. (2003) Variation of glucosinolate accumulation among different organs and developmental stages of *Arabidopsis thaliana*. *Phytochemistry* 62: 471–481.
- Burow, M. and Wittstock, U. (2009) Regulation and function of specifier proteins in plants. *Phytochem. Rev.* 8: 87–99.
- Chhajed, S., Misra, B.B., Tello, N. and Chen, S. (2019) Chemodiversity of the glucosinolate-myrosinase system at the single cell type resolution. *Front. Plant Sci.* 10: 618.
- Christianson, D.D., Cavins, J.F. and Wall, J.S. (1965) Steep liquor constituents. Identification and determination of nonprotein nitrogenous substances in corn steep liquor. *J. Agric. Food Chem.* 13: 277–280.
- Christianson, D.D., Wall, J.S. and Cavins, J.F. (1965) Nutrient distribution in grain. Location of nonprotein nitrogenous substances in corn grain. *J. Agric. Food Chem.* 13: 272–276.
- Clarke, D.B. (2010) Glucosinolates, structures and analysis in food. *Anal. Methods* 2: 310.
- Clay, N.K., Adio, A.M., Denoux, C., Jander, G. and Ausubel, F.M. (2009) Glucosinolate metabolites required for an *Arabidopsis* innate immune response. *Science* 323: 95–101.
- Falk, K.L., Tokuhisa, J.G. and Gershenzon, J. (2007) The effect of sulfur nutrition on plant glucosinolate content: physiology and molecular mechanisms. *Plant Biol.* 9: 573–581.
- Felle, H.H. (2001) pH: signal and messenger in plant cells. *Plant Biol.* 3: 577–591.
- Fujiwara, T., Hirai, M.Y., Chino, M., Komeda, Y. and Naito, S. (1992) Effects of sulfur nutrition on expression of the soybean seed storage protein genes in transgenic petunia. *Plant Physiol.* 99: 263–268.
- Gigolashvili, T., Yatushevich, R., Berger, B., Müller, C. and Flügge, U.-I. (2007) The R2R3-MYB transcription factor HAG1/MYB28 is a regulator of methionine-derived glucosinolate biosynthesis in *Arabidopsis thaliana*. *Plant J.* 51: 247–261.
- Grob, K. and Matile, P.H. (1979) Vacuolar location of glucosinolates in horseradish root cells. *Plant Sci. Lett.* 14: 327–335.
- Grubb, C.D. and Abel, S. (2006) Glucosinolate metabolism and its control. *Trends Plant Sci.* 11: 89–100.
- Halkier, B.A. and Gershenzon, J. (2006) Biology and biochemistry of glucosinolates. *Annu. Rev. Plant Biol.* 57: 303–333.
- Hanschen, F.S., Kaufmann, M., Kupke, F., Hackl, T., Kroh, L., Rohn, S., et al. (2018) Brassica vegetables as sources of epithionitriles: Novel secondary products formed during cooking. *Food Chem.* 245: 546–569.
- Hirai, M.Y., Fujiwara, T., Chino, M. and Naito, S. (1995) Effects of sulfate concentrations on the expression of a soybean seed storage protein gene and its reversibility in transgenic *Arabidopsis thaliana*. *Plant Cell Physiol.* 36: 1331–1339.
- Hirai, M.Y., Sugiyama, K., Sawada, Y., Tohge, T., Obayashi, T., Suzuki, A., et al. (2007) Omics-based identification of *Arabidopsis* Myb transcription factors regulating aliphatic glucosinolate biosynthesis. *Proc. Natl. Acad. Sci. USA* 104: 6478–6483.
- Hirai, M.Y., Yano, M., Goodenowe, D.B., Kanaya, S., Kimura, T., Awazuhara, M., et al. (2004) Integration of transcriptomics and metabolomics for understanding of global responses to nutritional stresses in *Arabidopsis thaliana*. *Proc. Natl. Acad. Sci. USA* 101: 10205–10210.
- Hooper, C.M., Stevens, T.J., Saukkonen, A., Castleden, I.R., Singh, P., Mann, G. W., et al. (2017) Multiple marker abundance profiling: combining selected reaction monitoring and data-dependent acquisition for rapid estimation of organelle abundance in subcellular samples. *Plant J.* 92: 1202–1217.
- Hooper, C.M., Tanz, S.K., Castleden, I.R., Vacher, M.A., Small, I.D. and Millar, A.H. (2014) SUBAcon: A consensus algorithm for unifying the subcellular localization data of the *Arabidopsis* proteome. *Bioinformatics* 30: 3356–3364.
- Ishida, M., Hara, M., Fukino, N., Kakizaki, T. and Morimitsu, Y. (2014) Glucosinolate metabolism, functionality and breeding for the improvement of Brassicaceae vegetables. *Breed. Sci.* 64: 48–59.
- Janowitz, T., Trompeter, I. and Piotrowski, M. (2009) Evolution of nitrilases in glucosinolate-containing plants. *Phytochemistry* 70: 1680–1686.
- Kataoka, T., Watanabe-Takahashi, A., Hayashi, N., Ohnishi, M., Mimura, T., Buchner, P., et al. (2004) Vacuolar sulfate transporters are essential

- determinants controlling internal distribution of sulfate in *Arabidopsis*. *Plant Cell* 16: 2693–2704.
- Katz, E., Nisani, S., Yadav, B.S., Woldemariam, M.G., Shai, B., Obolski, U., et al. (2015) The glucosinolate breakdown product indole-3-carbinol acts as an auxin antagonist in roots of *Arabidopsis thaliana*. *Plant J.* 82: 547–555.
- Kimura, Y., Ushiwatari, T., Suyama, A., Wada, R.T., Wada, T. and Maruyama-Nakashita, A. (2019) Contribution of root hair development to sulfate uptake in *Arabidopsis*. *Plants (Basel)* 8: 106.
- Koroleva, O.A. and Cramer, R. (2011) Single-cell proteomic analysis of glucosinolate-rich S-cells in *Arabidopsis thaliana*. *Methods* 54: 413–423.
- Kutz, A., Müller, A., Hennig, P., Kaiser, W.M., Piotrowski, M. and Weiler, E.W. (2002) A role for nitrilase 3 in the regulation of root morphology in sulphur-starving *Arabidopsis thaliana*. *Plant J.* 30: 95–106.
- Long, S.R., Kahn, M., Seefeldt, L., Tsay, Y.F. and Kopriva, S. (2015) Chapter 16 nitrogen and sulfur. In *Biochemistry & Molecular Biology of Plants*. Edited by Buchana, B.B., Gruissem, W., Jones, R.L. pp.746–768. Wiley Blackwell, Chichester.
- Malinovsky, F.G., Thomsen, M.-L.F., Nintemann, S.J., Jagd, L.M., Bourguine, B., Burow, M., et al. (2017) An evolutionarily young defense metabolite influences the root growth of plants via the ancient TOR signaling pathway. *eLife* 6: e29353.
- Maruyama-Nakashita, A. (2017) Metabolic changes sustain the plant life in low-sulfur environments. *Curr. Opin. Plant Biol.* 39: 144–151.
- Maruyama-Nakashita, A., Inoue, E., Watanabe-Takahashi, A., Yamaya, T. and Takahashi, H. (2003) Transcriptome profiling of sulfur-responsive genes in *Arabidopsis* reveals global effects of sulfur nutrition on multiple metabolic pathways. *Plant Physiol.* 132: 597–605.
- Maruyama-Nakashita, A., Nakamura, Y., Tohge, T., Saito, K. and Takahashi, H. (2006) *Arabidopsis* SLIM1 is a central transcriptional regulator of plant sulfur response and metabolism. *Plant Cell* 18: 3235–3251.
- Maruyama-Nakashita, A., Nakamura, Y., Watanabe-Takahashi, A., Inoue, E., Yamaya, T. and Takahashi, H. (2005) Identification of a novel cis-acting element conferring sulfur deficiency response in *Arabidopsis* roots. *Plant J.* 42: 305–314.
- Matile, P. (1980) The mustard oil bomb compartmentation of the myrosinase system. *Biochem. Physiol. Pflanz* 175: 722–731.
- Matsuda, F., Yonekura-Sakakibara, K., Niida, R., Kuromori, T., Shinozaki, K. and Saito, K. (2009) MS/MS spectral tag-based annotation of non-targeted profile of plant secondary metabolites. *Plant J.* 57: 555–577.
- Morikawa-Ichinose, T., Kim, S.J., Allahham, A., Kawaguchi, R. and Maruyama-Nakashita, A. (2019) Glucosinolate distribution in the aerial parts of *sel1-10*, a disruption mutant of the sulfate transporter SULTR1;2, in mature *Arabidopsis thaliana* plants. *Plants* 8: 95.
- Nakano, R.T., Piślewska-Bednarek, M., Yamada, K., Edger, P.P., Miyahara, M., Kondo, M., et al. (2017) PYK10 myrosinase reveals a functional coordination between endoplasmic reticulum bodies and glucosinolates in *Arabidopsis thaliana*. *Plant J.* 89: 204–220.
- Nikiforova, V., Freitag, J., Kempa, S., Adamik, M., Hesse, H. and Hoefgen, R. (2003) Transcriptome analysis of sulfur depletion in *Arabidopsis thaliana*: interlacing of biosynthetic pathways provides response specificity. *Plant J.* 33: 633–650.
- Nour-Eldin, H.H., Andersen, T.G., Burow, M., Madsen, S.R., Jørgensen, M.E., Olsen, C.E., et al. (2012) NRT/PTR transporters are essential for translocation of glucosinolate defence compounds to seeds. *Nature* 488: 531–534.
- Paulose, B., Chhikara, S., Coomey, J., Jung, H.-I., Vatamaniuk, O. and Dhankher, O.P. (2013) A γ -glutamyl cyclotransferase protects *Arabidopsis* plants from heavy metal toxicity by recycling glutamate to maintain glutathione homeostasis. *Plant Cell* 25: 4580–4595.
- Petersen, B., Chen, S., Hansen, C., Olsen, C. and Halkier, B. (2002) Composition and content of glucosinolates in developing *Arabidopsis thaliana*. *Planta* 214: 562–571.
- Salehin, M., Li, B., Tang, M., Katz, E., Song, L., Ecker, J.R., et al. (2019) Auxin-sensitive Aux/IAA proteins mediate drought tolerance in *Arabidopsis* by regulating glucosinolate levels. *Nat. Commun.* 10: 4021.
- Sessions, A., Burke, E., Presting, G., Aux, G., McElver, J., Patton, D., et al. (2002) A high-throughput *Arabidopsis* reverse genetics system. *Plant Cell* 14: 2985–2994.
- Shimada, T., Takagi, J., Ichino, T., Shirakawa, M. and Hara-Nishimura, I. (2018) Plant vacuoles. *Annu. Rev. Plant Biol.* 69: 123–145.
- Sønderby, I.E., Geu-Flores, F. and Halkier, B.A. (2010) Biosynthesis of glucosinolates—gene discovery and beyond. *Trends Plant Sci.* 15: 283–290.
- Takahashi, H., Kopriva, S., Giordano, M., Saito, K. and Hell, R. (2011) Sulfur assimilation in photosynthetic organisms: molecular functions and regulations of transporters and assimilatory enzymes. *Annu. Rev. Plant Biol.* 62: 157–184.
- Talalay, P. and Fahey, J.W. (2001) Phytochemicals from cruciferous plants protect against cancer by modulating carcinogen metabolism. *J. Nutr.* 131: 3027S–3033S.
- Tanz, S.K., Castleden, I., Hooper, C.M., Vacher, M., Small, I. and Millar, H.A. (2013) SUBA3: a database for integrating experimentation and prediction to define the SUBcellular location of proteins in *Arabidopsis*. *Nucleic Acids Res.* 41: D1185–D1191.
- Traka, M. (2016) Health Benefits of Glucosinolates. *Adv. Bot. Res.* 80: 247–279.
- Traka, M. and Mithen, R. (2009) Glucosinolates, isothiocyanates and human health. *Phytochem. Rev.* 8: 268–282.
- Wittstock, U. and Burow, M. (2010) Glucosinolate breakdown in *Arabidopsis*: mechanism, regulation and biological significance. *Arabidopsis Book* 8: e0134.
- Wittstock, U., Meier, K., Dörr, F. and Ravindran, B.M. (2016) NSP-dependent simple nitrile formation dominates upon breakdown of major aliphatic glucosinolates in roots, seeds, and seedlings of *Arabidopsis thaliana* Columbia-0. *Front. Plant Sci.* 7: 1821.
- Xu, Z., Escamilla-Treviño, L., Zeng, L., Lalgondar, M., Bevan, D., Winkel, B., et al. (2004) Functional genomic analysis of *Arabidopsis thaliana* glycoside hydrolase family 1. *Plant Mol. Biol.* 55: 343–367.
- Yamaguchi, C., Takimoto, Y., Ohkama-Ohtsu, N., Hokura, A., Shinano, T., Nakamura, T., et al. (2016) Effects of cadmium treatment on the uptake and translocation of sulfate in *Arabidopsis thaliana*. *Plant Cell Physiol.* 57: 2353–2366.
- Zhang, Z., Ober, J.A. and Kliebenstein, D.J. (2006) The gene controlling the quantitative trait locus EPITHIOSPECIFIER MODIFIER1 alters glucosinolate hydrolysis and insect resistance in *Arabidopsis*. *Plant Cell* 18: 1524–1536.
- Zhou, C., Tokuhisa, J.G., Bevan, D.R. and Esen, A. (2012) Properties of β -thioglucoside hydrolases (TGG1 and TGG2) from leaves of *Arabidopsis thaliana*. *Plant Sci.* 191–192: 82–92.